Baileychlore, the Zn end member of the trioctahedral chlorite series

Audrey C. Rule

Department of Geology and Geophysics, University of Wisconsin, Madison, Wisconsin 53706, U.S.A.

Frank Radke

Australian Mineral Development Laboratories, Frewville, South Australia, 5063, Australia

Abstract

Baileychlore occurs as dark green rims on colloform calcite veins within a strongly oxidized collapse karst–breccia containing altered andesite and garnet-vesuvianite skarn clasts at the Red Dome deposit near Chillagoe, Queensland, Australia. Baileychlore is a new Zn-rich chlorite. The ZnO contents are fairly uniform from 28.2 to 30.5 wt% at a depth of 89.6 m in the deposit, with a structural formula of $(Zn_{2.50}Fe^{2+}_{1.20}Al_{1.17}Mg_{0.76}Mn^{2+}_{0.01}\square_{0.36})(Si_{3.55}Al_{0.45})O_{10}(OH)_8$ for the most Zn-rich analysis. The name is for Professor Sturges W. Bailey of the University of Wisconsin and is to be used for any trioctahedral chlorite in which Zn is the dominant divalent octahedral cation.

Baileychlore occurs as fine-grained transverse fibers exhibiting zoned pleochroic colors (green to yellow-green) along their length. Refractive indices are $\alpha = 1.582$ and $\gamma = 1.614$. The measured and calculated densities are 3.18(2) and 3.195 g/cm³, respectively. Combined DTA-TGA curves show a major endotherm at 550 °C, a small, double-bottomed endotherm in the range 680–750 °C, and an exotherm at 850 °C. The X-ray powder pattern is that of the Ib ($\beta = 97°$) polytype. The strongest lines (24 given) are $[d_{obs}(I_{obs})(hkl)]$ 14.3(90)(001), 7.14(100)(002), 4.600(30)(02;11), 3.573(40)(004), 2.660(50)(20$\bar{1}$,130), 2.450(35)(20$\bar{3}$,132), and 1.542(60)(060,331). Unit-cell dimensions are $a = 5.346(3)$, $b = 9.257(4)$, $c = 14.401(7)$ Å, and $\beta = 97.12(5)°$. The symmetry is probably triclinic $C\bar{1}$ or $C1$ because of semi-random stacking. A one-dimension electron-density projection and an asymmetry value of $+1.29$ suggest a composition $(Zn_{2.50}Al_{0.14}\square_{0.36})^{0.58-}$ for the octahedral sheet within the 2:1 layer and $(Fe^{2+}_{1.20}Al_{1.03}Mg_{0.76}Mn^{2+}_{0.01})^{1.03+}$ for the interlayer sheet.

Introduction

Radke et al. (1978) reported chlorite containing 6 to 30 wt% ZnO from a drillhole located near Chillagoe, Australia. Frondel and Ito (1975) previously described a zincian, manganoan "brunsvigite" (chamosite in the preferred nomenclature of Bayliss, 1975) containing 9.60 wt% ZnO and 9.96 wt% MnO from Franklin, New Jersey, and Dunn et al. (1987) described the chlorite isotype franklinfurnaceite from the same general area as a new species with up to 24 wt% ZnO (primarily tetrahedral), 19 wt% MnO, and 10% Mn₂O₃. The Australian occurrence is the only chlorite known to date, however, in which Zn is the dominant divalent octahedral cation present. The ZnO contents range from 22 to 30 wt% for these latter specimens. The present paper provides a name and additional crystallographic and structural data for this species.

The mineral has been named baileychlore in honor of Professor Sturges W. Bailey of the Department of Geology and Geophysics, University of Wisconsin, Madison. Professor Bailey is well known for his research on the structures and polytypism of chlorites, and he was the first to recognize the structural type to which these particular Zn-rich specimens belong. Following the nomenclature of Bayliss (1975), baileychlore is to be used as the name for

the Zn end member of the trioctahedral chlorite series, ideally $(Zn_5Al)(Si_3Al)O_{10}(OH)_8$, or for any trioctahedral chlorite in which Zn is the dominant divalent octahedral cation. The name is analogous to clinochlore, the Mg end member. The mineral and name were approved prior to publication by the IMA Commission on New Minerals and Mineral Names. Holotype material has been deposited with the Smithsonian Institution (NMNH 164430), the South Australian Museum (no. 13592), and the Geology Museum at the University of Wisconsin, Madison (no. 6000/1).

Occurrence, Morphology, and Origin

Baileychlore is known only from one angled drillhole (DDH2) drilled in 1972 to test beneath the Red Dome deposit. The Red Dome deposit is located near Mungana approximately 15 km west-northwest of Chillagoe, North Queensland, and is being developed as a gold mine by Elders Resources Ltd. The drillhole extends 180 m and intersects an assemblage of brecciated and highly altered andesites and garnet-vesuvianite skarns. Chlorite has pervasively replaced the andesites and some of the skarns, calcite has replaced garnet-rich skarns, and at depths below about 120 m, silicification and alteration to iron ox-
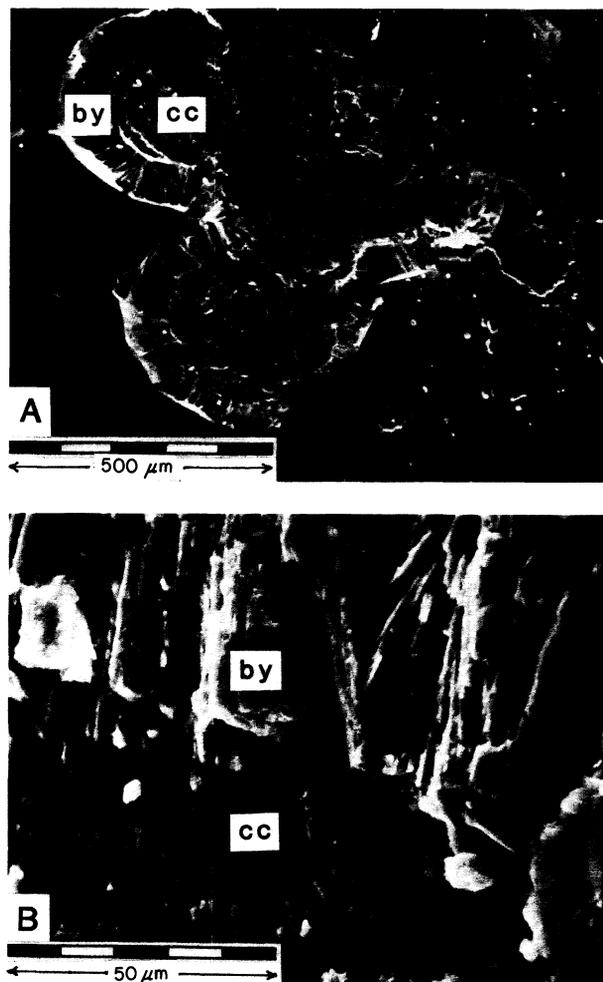
Fig. 1. SEM photographs of (A) Baileychlore (by) rims on colloform calcite (cc) veinlets. (B) Transverse fibers of baileychlore (by) adjacent to calcite (cc) vein.

ides are extensive. Below about 50 m the samples have a fairly uniform ZnO content between 4 and 6 wt% with most or all of the Zn in Zn-bearing chlorites. Most of the results presented in this paper are from pleochroic, dark green chlorite rims on colloform calcite veins occurring within the breccia at a depth of 89.6 m. This chlorite has the highest ZnO content noted (28 to 30 wt%) and at high magnifications (Fig. 1) can be seen to form fine transverse fibers about 3–10 μm in diameter. Native copper is generally intergrown with the calcite and fibrous baileychlore.

The Red Dome breccia is interpreted by Smith (1985) and Torrey et al. (1986) to be a collapse karst–breccia formed under weathering conditions by solution of marble by meteoric water. The rock types forming the breccia clasts include skarn, andesite, quartzofeldspathic sandstone, felsic porphyries, and chert; the clasts range in size from a few millimeters to 70 m. The matrix is generally limonitic, goethitic, or chloritic and includes finely laminated sandstones deposited by meteoric ground water.

Cementing minerals include goethite, hematite, chalcocite, malachite, cuprite, native copper, and calcite.

Chlorite occurs as matrix material and as a replacement of andesite and skarn clasts. This chlorite is a zincian chamosite. Zincian chamosite from the collapse karst–breccia is also reported by Smith (1985). Baileychlore, as distinct from zincian chamosite, has only been identified in dark green, fibrous veinlets up to 1 mm wide that commonly form on the margins of calcite veins.

The primary base- and precious-metal mineralization at Red Dome is associated with calcsilicate skarns and includes bornite, sphalerite, and various tellurides, including gold and gold-silver tellurides (Torrey et al., 1986). The zinc chlorites, including baileychlore, have formed by crystallization of remobilized elements of the primary minerals during weathering by meteoric ground water. Details of this process are discussed by Smith (1985).

Chemistry

Table 1 presents 12 electron-microprobe point analyses by Radke et al. (1978) for chlorite from four different depths. Analyses 3 to 8 are for the fibrous baileychlore at a depth of 89.6 m. The ZnO contents of these latter analyses are fairly uniform from 28.2 to 30.5 wt%. Allocations of the analyses to the site occupancies shown in Table 1 are based on 14 oxygen atoms, assuming 8 OH and all Fe to be ferrous on the basis of qualitative microchemical tests. Analysis 8 for the most Zn-rich specimen gives a formula $(Zn_{2.48}Fe^{2+}_{1.19}Al_{1.13}Mg_{0.75}Mn^{2+}_{0.01}Ca_{0.12}\square_{0.32})(Si_{3.52}Al_{0.48})$ $O_{10}(OH)_8$. In samples of low ZnO content, the deficiency in Zn is compensated for by additional Fe^{2+}, and the chlorite is properly termed zincian chamosite. Baileychlore has an appreciable dioctahedral component in that about 0.3 of the 6 octahedral sites are vacant.

All of the analyses show 0.2 to 1.0% CaO. It is not known for certain if this is due to calcite impurities or to Ca in the structure. Ca is not believed to substitute easily into the chlorite structure, although it is present as an essential component in the hybrid chlorite-mica structure of franklinfurnaceite (Dunn et al., 1987), and there is calcite closely associated with the baileychlore. If Ca is excluded from the structure, the formula unit for analysis 8 becomes $(Zn_{2.50}Fe^{2+}_{1.20}Al_{1.17}Mg_{0.76}Mn^{2+}_{0.01}\square_{0.36})(Si_{3.55}Al_{0.45})$- $O_{10}(OH)_8$. The tetrahedral Al content of baileychlore is 0.44 to 0.49 atoms (Table 1), which is near the lower limit for the chlorite structure but is characteristic of the structural form (Ib, $\beta = 97°$) of baileychlore. The structural formula suggests that the octahedral sheet within the 2:1 layer also has a net negative charge, because of the presence of vacancies, and that the total layer charge is approximately -1.0. The MnO content is low, 0.4% or less for all specimens analyzed, and is in contrast to the high values reported for the zincian chlorites from Franklin, New Jersey (Frondel and Ito, 1975; Dunn et al., 1987).

Physical properties

It was not possible to obtain complete optical properties because of the fine grain size and fibrous character of

TABLE 1. Electron-microprobe analysis of chlorites (wt%)

	Depth											
	51.5 m (169 ft)		89.6 m (294 ft)						96.7 m (317 ft)			97.6 m (320 ft)
Sample:	1	2	3	4	5	6	7	8	9	10	11	12
SiO_2	24.4	27.3	32.1	31.8	32.4	32.1	32.0	32.0	25.6	25.3	26.2	27.4
TiO_2	0.6	0.6	n.d.	n.d.	n.d.	n.d.	n.d.	n.d.	0.6	0.4	0.14	0.2
Al_2O_3	17.9	19.6	12.5	12.6	12.4	12.5	12.9	12.4	15.8	18.3	16.0	16.8
FeO*	29.8	22.5	14.5	14.1	13.7	13.5	12.5	12.9	26.7	22.9	17.6	25.4
MnO	0.1	0.4	0.15	0.13	0.16	0.14	0.13	0.15	0.15	0.16	0.1	0.15
MgO	6.4	4.7	4.7	4.7	4.5	4.6	4.4	4.6	6.4	6.2	5.1	5.3
CaO	0.2	0.5	0.9	0.9	1.0	0.9	1.0	1.0	0.4	0.3	0.5	0.45
ZnO	6.0	10.7	28.2	28.8	29.1	29.4	30.4	30.5	14.2	14.4	22.6	14.5
Total	85.4	85.8	93.1	93.0	93.3	93.1	93.3	93.5	89.8	88.0	88.2	90.2

Number of cations on the basis of $O_{10}(OH)_8$

Tetrahedral cations ($\Sigma = 4$)

	1	2	3	4	5	6	7	8	9	10	11	12
Si	2.838	3.087	3.528	3.512	3.558	3.528	3.517	3.524	2.919	2.876	3.046	3.067
Al	1.162	0.913	0.472	0.488	0.442	0.472	0.483	0.476	1.081	1.124	0.954	0.933

Octahedral cations

	1	2	3	4	5	6	7	8	9	10	11	12
Al	1.283	1.695	1.143	1.146	1.160	1.154	1.193	1.127	1.043	1.333	1.235	1.275
Zn	0.517	0.897	2.293	2.343	2.361	2.389	2.468	2.478	1.192	1.208	1.940	1.196
Fe	2.893	2.126	1.331	1.300	1.261	1.245	1.145	1.187	2.543	2.184	1.707	2.375
Mg	1.100	0.785	0.775	0.767	0.731	0.748	0.714	0.751	1.082	1.058	0.883	0.883
Mn	0.012	0.037	0.014	0.012	0.015	0.013	0.012	0.014	0.015	0.016	0.010	0.014
Ca	0.028	0.062	0.110	0.105	0.114	0.112	0.114	0.118	0.049	0.034	0.061	0.035
Ti	0.054	0.005	—	—	—	—	—	—	0.049	0.033	0.012	0.017
Total	5.89	5.61	5.67	5.67	5.64	5.66	5.65	5.68	5.97	5.87	5.85	5.82

Note: Analyst was P. K. Schultz. Modified from Radke et al. (1978). Analyses 3 to 8 are of fibrous baileychlore; others are of zincian chamosite; n.d. = not determined.
* Total Fe as FeO.

baileychlore. The mean refractive index is about 1.59. Values of $\alpha = 1.582$ and $\gamma = 1.614$ were measured for baileychlore from the 89.6-m depth. The chlorite fibers exhibit a zoned pleochroic color with the zoning parallel to the chlorite veins (zoned along the length of the fibers) to produce a colloform-type banding. The zoning is in shades of green and yellow-green. The pleochroism is weak with the strongest colors in the darker bands. The measured density of baileychlore from the 89.6-m depth is 3.18(2), which compares favorably with a calculated density of 3.195 g/cm^3 for the most Zn-rich material of analysis 8 (Table 1).

Simultaneous DTA and TGA runs were carried out using a Rigaku Denki model M8076 instrument. A 50-mg sample of hand-picked and finely ground baileychlore was used, with an equal amount of calcined alumina as reference. The heating rate was 10 °C/min in a static atmosphere of air. The principal thermal effects (Fig. 2) and their interpretations are as follows: (1) Ambient to 120 °C: A small broad endotherm accompanied by a loss of moisture (~3% wt loss). (2) 150–200 °C: A very small DTA endotherm and weight loss attributed to loosely combined water. (3) 280–330 °C: A very small DTA endotherm and weight loss probably due to a trace of goethite contaminant. (4) 400–600 °C: A major DTA endotherm and weight loss due to dehydroxylation of the interlayer sheet of chlorite. (5) 680–750 °C: A very small, broad, double-bottomed endotherm and corresponding weight loss due to dehydroxylation of the 2:1 layer of chlorite. (6) 780–880 °C: A broad exothermic DTA peak with no weight loss.

This is attributed to formation of a high-temperature aluminosilicate phase from the decomposed chlorite at about 850 °C. (7) 1000–1200 °C: The DTA curve shows an increasing endothermic band with significant weight loss. This is probably due to sintering of the sample, which exhibited pronounced shrinkage.

The major feature of the DTA curve is the dehydroxylation of the interlayer sheet at 550 °C. The dehydroxylation of the 2:1 layer is less well defined in the range 680–750 °C, and it is likely that some of its dehydration is included in the 550 °C endotherm. The endotherms in general are not as sharp as those from well-crystallized trioctahedral chlorites and occur at lower temperatures, presumably because of poorer crystallinity and consequent release of water more readily and over a large range of temperature. The presence of octahedral vacancies in baileychlore (Table 1) also may affect the curve. Müller (1963) noted a large endotherm at 544 °C and two small endotherms at 680 and 725 °C for dioctahedral chlorite.

STRUCTURAL DATA

Baileychlore is poorly crystalline and gives X-ray powder patterns in which the *hkl* peaks are broad. Both Debye-Scherrer and diffractometer patterns (Table 2) taken with graphite-monochromated $FeK\alpha$ and $CuK\alpha$ X-radiation are recognizable as being characteristic of the Ib ($\beta = 97°$) polytype as defined by Bailey and Brown (1962). In this polytype the interlayer sheet is oriented so that its slant is in the same direction as that of the octahedral sheet within the 2:1 layer. The interlayer is positioned asym-
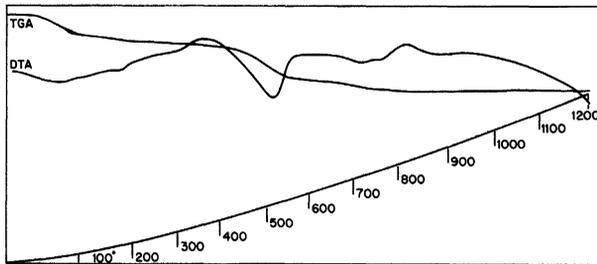
Fig. 2. Combined DTA-TGA curves for baileychlore.

Fig. 3. One-dimensional electron-density projection using seven 00*l* reflections. The unlabeled peak at $z = 0.35$ is a diffraction ripple.

metrically for hydrogen bonding so that is has a *b* position relative to the 2:1 layer on one side but an *a* position relative to the layer on the other side. The presence of the I*b* ($\beta = 97°$) polytype is consistent with the composition and mode of origin of this chlorite. Bailey and Brown (1962) considered the I*b* ($\beta = 97°$) polytype to be the least stable of the four chlorite structures known at that time, to form at the lowest temperature, and to have the smallest substitution of tetrahedral Al for Si.

Cell dimensions derived by least-squares refinement of the X-ray powder data are $a = 5.346(3)$, $b = 9.257(4)$, $c = 14.401(7)$ Å, and $\beta = 97.12(5)°$. Although single crystals are not available, the shapes of the powder-diffraction peaks at $d = 4.600$ and 1.745 Å are suggestive of two-

TABLE 2.   Baileychlore X-ray powder data

hkl	I_{obs}	d_{obs} (Å)	d_{calc} (Å)
001	90	14.3	14.290
002	100	7.14	7.145
003	5	4.76	4.763
02;11*	30	4.600	4.628 / 4.602
004	40	3.573	3.572
005	10	2.860	2.858
20$\bar{1}$ 130	50	2.660	2.668 / 2.667
20$\bar{2}$ 131	5	2.59	2.594 / 2.593
20$\bar{3}$ 132	35	2.450	2.450 / 2.449
20$\bar{4}$, 133	2	2.27	2.268
20$\bar{5}$ 134	15	2.080	2.078 / 2.076
007	2	2.040	2.041
20$\bar{6}$, 135	2	1.89	1.892
15;24;31*	20	1.745	1.748 / 1.737
207, 136	10	1.722	1.724
060, 33$\bar{1}$	60	1.542	1.543
062, 33$\bar{3}$, 331	25	1.508	1.508
20$\bar{9}$, 138	10	1.44	1.443
00.10	3	1.428	1.429
064, 33$\bar{5}$, 333	15	1.415	1.416
065, 33$\bar{6}$, 334	1	1.36	1.358
26$\bar{1}$ 40$\bar{2}$, 260	20	1.335	1.336 / 1.334
40$\bar{4}$ 262	20	1.295	1.297 / 1.296
20.10;13.$\bar{1}\bar{1}$	2	1.198	1.198

Note: Monochromatic Fe$K\alpha$ radiation. Camera diameter 114.6 mm. Intensities estimated visually. B = broad peak.
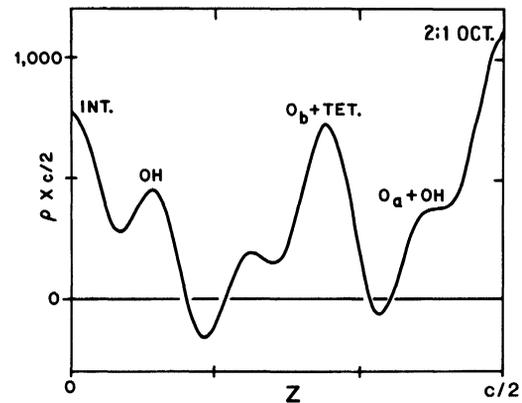* Two-dimensional band.

dimensional bands and thus of semirandom stacking of adjacent layers and interlayers. This is true also for all single crystals studied to date of both I*b* ($\beta = 97°$) and I*b* ($\beta = 90°$) chlorite from other localities. Bailey and Brown (1962) considered the symmetry of all chlorites with semirandom stacking to be triclinic, $C1$ or $C\bar{1}$.

It did not prove possible to make an oriented-clay slide by settling from a liquid suspension or by suction through ceramic tile, even for every dilute suspension after disaggregation by ultrasonic treatment. This is probably due to the fibrous nature of baileychlore. The integrated intensities of seven nonoverlapped basal reflections were measured from an unoriented slide using a Philips X-ray diffractometer with graphite-monochromated Cu$K\alpha$ radiation and a sequence of ¼° to 1° vertical divergence slits. The intensities were corrected for the Lp factor for randomly oriented crystallites, converted to F values, and used to construct a 1-dimensional electron-density projection (Fig. 3). Because the two octahedral sheets in the chlorite structure are separated by $c/2$, all octahedral cations diffract in phase with one another for even orders of 00*l* regardless of the distribution of cations between the two sheets. Comparison of the sum of these observed F values with a similar sum calculated for the octahedral composition of baileychlore yields a scaling factor to place the observed values on an absolute scale.

The peak for the octahedral cations within the 2:1 layer at $z = \frac{1}{2}$ in Figure 3 has greater electron density that that for the octahedral cations of the interlayer sheet at $z = 0$. Integration of the areas of these two peaks and scaling relative to a content of 27 electrons for the resolved interlayer OH plane gives a total of 116 electrons, which may be compared with 125 electrons for the octahedral cation total of analysis 8 of Table 1 (assuming 50% ionization). The excess of electron density in the 2:1 layer is 27 electrons (9 electrons per cation). These electron-density values should not be considered accurate because of the availability of only seven 00*l* reflections and the consequent presence of Fourier termination effects. The data

are internally consistent, however, because the heavy-atom asymmetry calculated from the 00l intensities is +1.29. This means that there are 1.29 more heavy atoms of Zn + Fe in the 2:1 layer than in the interlayer. For this calculation the method of Petruk (1964) was modified by construction of a graph appropriate for an average heavy atom of $Zn_{0.67}Fe_{0.33}$.

It is not possible with these data to give an unequivocal distribution of the octahedral cations over the two octahedral sheets. However, if the vacancies are in the *trans* M(1) sites of the 2:1 layer, as in most layer silicates, it is more likely that the heavier Zn ($Z = 30$ vs. $Z = 26$ for Fe) would also be in the 2:1 layer. There is no evidence for tetrahedral Zn from Figure 3, in contrast to the Si_2Zn_2 tetrahedral composition found in franklinfurnaceite by Dunn et al. (1987). A reasonable cation distribution for the composition of analysis 8 that satisfies both the observed asymmetry and the electron-density values is $(Zn_{2.50}Al_{0.14}\square_{0.36})^{0.58-}$ for the octahedral sheet of the 2:1 layer and $(Fe^{2+}_{1.20}Mn^{2+}_{0.01}Al_{1.03}Mg_{0.76})^{1.03+}$ for the interlayer sheet. This gives an asymmetry of +1.29 for the heavy atoms with 23 more electrons in the octahedra of the 2:1 layer. The net negative charge of 0.45 on the tetrahedral sheets is augmented by a negative charge of 0.58 on the octahedral sheet for this distribution to give a net charge of −1.03 for the 2:1 layer as a whole. However, it must be emphasized that other cation distributions are possible and that resolution of the problem requires a larger number of 00l intensities.

ACKNOWLEDGMENTS

REFERENCES